Impact of fluorinated vinylene units on supramolecular organization and optical properties of poly(p-phenylenedifluorovinylene) thin films as a class of blue band gap conjugated polymers

Maria Losurdo [a], Maria M. Giangregorio [a], Pio Capezzuto [a,b], Giovanni Bruno [a,*], Francesco Babudri [b,c], Antonio Cardone [c], Carmela Martinelli [b], Gianluca M. Farinola [b,c], Francesco Naso [b,c], Michael Büchel [d]

[a] Institute of Inorganic Methodologies and of Plasmas, IMIP-CNR, via Orabona 4, 70126 Bari, Italy
[b] Dipartimento di Chimica, Università degli Studi di Bari, via Amendola 168, 70126 Bari, Italy
[c] Istituto di Chimica dei Composti Organometallici, ICCOM-CNR di Bari, via Orabona 4, 70126 Bari, Italy
[d] Philips Technologie GmbH BCA Aachen, Philipsstrasse 8, Gebäude VM202, D-52068 Aachen, Germany

ABSTRACT

This study is an investigation on the interplay between supramolecular organization and optical properties of thin films of conjugated polymers with fluorinated vinylene units such as poly[2-(2-ethyl-hexyloxy)-5-methoxy]-1,4-phenylenedifluorovinylene (MEH-PPDFV) and poly(2-methoxy-5-propyl-oxysulfonatephenylenedifluorovinylene) (MPS-PPDFV), which are both PPV polymers with fluorinated double bonds with alkoxy chains in the 2 and 5 positions. MEH-PPDFV is the fluorinated version of the widely investigated MEH-PPV, and MPS-PPDFV is characterized by the presence of ionic alkoxy side chains. This interplay is elucidated exploiting atomic force microscopy, spectroscopic ellipsometry and photoluminescence to obtain complementary information. It is demonstrated that the presence of F-atoms in the vinylene units of the MEH-PPDFV yields a blue optical band gap with the maximum of the fundamental HOMO–LUMO transition and of the room temperature photoluminescence at 3.74 eV (331 nm) and at 2.71 eV (458 nm), respectively. The blue-absorption and emission in the thin films are ascribed to the fact that fluorine atoms on the vinylene units prevent π-stacking of polymeric chains. Furthermore, the dependence of morphology, anisotropy in optical properties and photoluminescence properties of films on deposition methodology is also discussed. MEH-PPDFV also emits homogeneous blue-greenish electroluminescence at 2.46 eV (504 nm).

1. Introduction

There has been growing interest in the development of polymeric semiconductors because they are versatile materials for flexible electronic and optoelectronic devices such as organic thin film transistors (OTFTs) and organic light-emitting diodes (OLEDs) [1,2]. Poly(p-phenylenevinylenes) (PPVs) are one of the most representative classes of semiconductor polymers for electroluminescent devices. While yellow-green and orange-red emissions have been obtained from PPV derivatives, examples of deep-blue emitting PPV polymers are quite rare. The yellow-green emission of unsubstituted PPV is shifted to the blue-green region by steric effects that twist the conjugated backbone, as in the case of some 2,3-dialkoxy substituted derivatives [3,4]. A more marked shift towards short wavelength emission has been reported for

2,3-diphenyl-5-alkyl derivatives [5,6]. The introduction of *meta* or *ortho* phenylene units in the main chain is also effective in blue-shifting the electroluminescence of simple dialkoxy PPV [7].

In this context, the introduction of electron-withdrawing substituents, and in particular of fluorine atoms, in the conjugated backbone has been shown to lower both the HOMO and the LUMO levels, thus affecting the band gap value, the emission properties and the electron injection properties of PPV polymers [7–9]. PPVs with fluorine atoms on the aromatic rings have been reported [8,10–14], whose absorption spectra in solution show a blue-shift with respect to the non-fluorinated counterparts, although the effect on photo- (PL) and electroluminescence (EL) is not in the same direction and marked red-shifts are observed [15–17].

Recently, PPV polymers with fluorinated vinylene units have been synthesized [18–20] as a class of polymers with increased stability to double bond photooxidation [21]. Indeed, poly(p-phenylenedifluorovinylene) (PPDFV) polymers, with two fluorine atoms on the vinylene units, have also been reported blue-shifting the absorption maximum to 390 nm [19]. Nevertheless, Jin et al.

* Corresponding author. Tel.: +39 0805442094; fax: +39 0805442024.
E-mail address: giovanni.bruno@ba.imip.cnr.it (G. Bruno).

[20,22] reported that films of PPDFV showed a red-shift of the emission to 580 nm, unless a bulky trialkylsilyl substituent on the *ortho* position to the double bond is present in addition to the fluorine atoms on the vinylene unit, i.e., the DMOS-PPDFV, poly(2-dimethyloctylsilyl-*p*-phenylenedifluorovinylene) [20,22], with a PL peaked at 495 nm, which is blue-shifted of 30 nm only with respect to the non-fluorinated polymer. This blue-shift was attributed to a reduction of the effective conjugation length by steric repulsion between the fluorine atoms on the double bonds and the bulky silyl group in the 2 position of the aromatic ring. Interestingly, DMOS-PPDFV has been demonstrated to yield high performance OLEDs, with efficiency being 7 times higher than that of the DMOS-PPV OLED [20,22]. These results motivate further investigation of PPVs with fluorinated vinylene units in order to better understand the role of fluorine atoms on vinylene units and of the chain side group on the optical properties of the PPDFV polymer thin films.

In this paper, we present results on thin films of fluorinated vinylene unit-based polymers, specifically poly[2-(2-ethylhexyl-oxy)-5-methoxy]-1,4-phenylenedifluorovinylene (MEH-PPDFV), demonstrating that the fluorine atoms on the PPVs' vinylene units represent a valuable structural modification to obtain films with the optical gap strongly blue-shifted to value as high as 3.7 nm (331 nm). With respect to previous works from Jin et al. [19,20,22] we show that films of MEH-PPDFV emit efficiently at room temperature in the blue region at 458 nm, which is blue-shifted of 200 nm with respect to the PL of the corresponding non-fluori-nated polymeric films. Besides the MEH-PPDFV, an alkoxy substituted polymer with a ionic sulfone group attached to the alkyl chains is also discussed, poly(2-methoxy-5-propyloxysulfonate-phenylenedifluorovinylene) (MPS-PPDFV), in order to study the effect of this ionic moiety on aggregation features of fluorinated PPV polymers. The focus is on the impact of fluorinated vinylene units on morphology and aggregation in the solid state and on optical properties of PPDFV thin films. Films have been deposited by spin coating and drop casting to obtain different film microstructures and morphologies, as detected by atomic force microscopy (AFM), while spectroscopic ellipsometry (SE) and photoluminescence (PL) have been used to monitor changes in

optical properties. Spectroscopic ellipsometry is also used to discuss the anisotropy and birefringence of thin films in relation to the polymer backbone, aggregation and morphology. Anisotropy of polymeric thin films is important for accurate design of devices, which requires knowledge of the energy dispersion of the complex refractive index, $N = n + ik$ (where n is the real refractive index and k is the extinction coefficient) of films. In fact, the energy dispersion of N affects the quantum efficiency and light extraction [23]. Furthermore, the optical anisotropy is strictly connected with the order of polymeric chains in the film [24]. Therefore, from the analysis of optical anisotropy, the degree of order of polymer chains, which depends on film formation conditions can be deduced. Finally, we also present preliminary data on the electro-luminescence of MEH-PPDFV films, although study is in progress on this last aspect through film optimization.

2. Experimental methods

2.1. Polymer synthesis

Polymers were synthesized by the Stille cross-coupling reaction [18], as schematized in Fig. 1; the non-fluorinated MEH-PPV was also prepared by the same way as comparison material. Our approach was to compare materials obtained by applying the same synthetic route, although polymers with different molecular weights, M_w, as also indicated in Fig. 1 were obtained, being one order of magnitude higher for the fluorinated polymers. Yields of the Stille cross-coupling reactions were quite high for MEH-PPDFV as also indicated in Fig. 1 and well reproducible.

2.2. Film preparation

Polymer films have been deposited on Corning glass by spin coating and by casting a chloroform solution by very slowly evap-orating the solvent while the whole system is kept inside a small box saturated by the vapor of the same solvent. All polymer solu-tions have been filtered before the deposition using a Teflon filter in PTFE with pore of 0.2 μm. A solution of 11 mg/ml in chloroform was
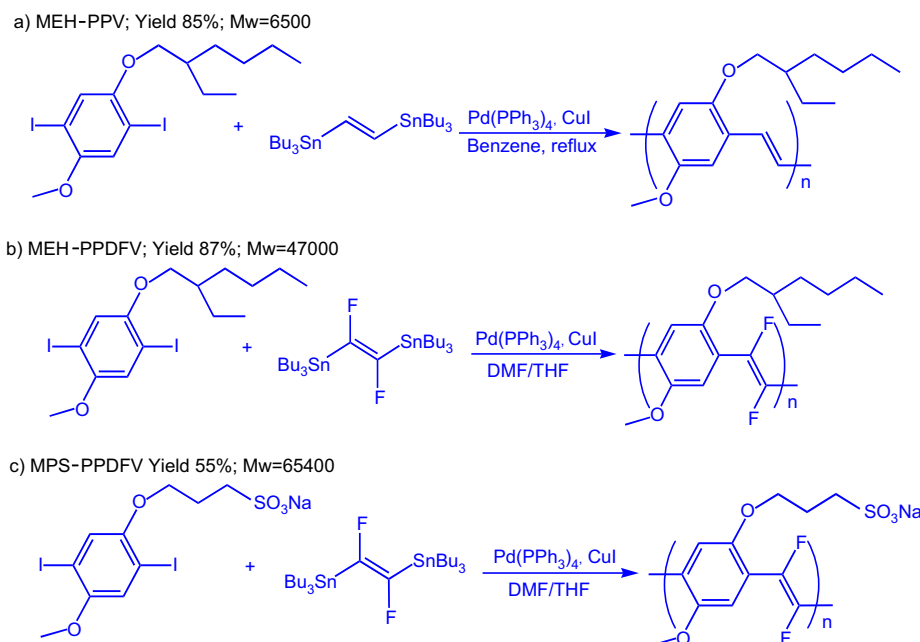

Fig. 1. Synthesis and formula of (a) MEH-PPV ($M_w = 6500$ g/mol), (b) MEH-PPDFV ($M_w = 47{,}000$ g/mol) and (c) MPS-PPDFV ($M_w = 65{,}400$ g/mol).

used for the MEH-PPDFV and MEH-PPV polymers, while a 5 mg/ml in DMSO solution was used for the MPS-PPDFV polymer.

Before analysis, all films have been annealed for 30 min at 130 °C in UHV to remove any residual solvent and stabilize film microstructure.

2.3. Characterization methods

The polymers in solution were analyzed by recording room temperature UV–vis spectra in a Shimadzu UV-2401 PC spectrophotometer and fluorescence spectra in a Varian Cary Eclipse fluorescence spectrophotometer.

The optical response of films was investigated by spectroscopic ellipsometry [25,26]. Measurements at multiple angles of incidence in the range 55°–70° were carried out to check anisotropy in optical properties using a phase modulated spectroscopic ellipsometer in the energy photon range 0.75–6.5 eV (UVISEL, Jobin Yvon) with a resolution of 0.01 eV. To derive the spectral dependence of $(n + ik)$ from the measured variable angle SE spectra of the pseudorefractive index, the experimental SE spectra of the pseudorefractive index, $\langle N \rangle$, and/or pseudodielectric function, $\langle \varepsilon \rangle = \langle \varepsilon_1 \rangle + i \langle \varepsilon_2 \rangle = \langle N \rangle^2$, were analyzed using a two-layer model consisting in substrate/ polymer film/surface roughness. The energy dispersion of the polymer optical constants was modeled using an ensemble of 4 Lorentzian oscillators:

$$N^2 = (n + ik)^2 = \varepsilon = \varepsilon_1 + i\varepsilon_2 = \varepsilon_\infty + \sum_j \frac{A_j \omega_j^2}{\omega_j^2 - \omega^2 - i\gamma_j \omega} \quad (1)$$

where ε_∞ is the high-frequency dielectric constant, ω_j, γ_j and A_j are the frequency, width and strength of the j oscillator. Four Lorentzian oscillators were considered on the basis of the band diagram reported for PPVs [27,28] including both delocalized (D, D*) bands and localized (L, L*) states. According to the band diagram, 4 main transitions are expected, in the investigated photon energy range, i.e., the HOMO D1 and LUMO D1* band at lower energy, the transition between localized and delocalized levels (L–D*) and (D–L*) generating a central band in the rang 4.5–5 eV, another transition due to the electron and hole states of a tightly bound Frenkel exciton localized on the phenyl ring (L–L*) at an energy of approximately 6–6.2 eV, and another peak at 3.7–4 eV of exciton origin.

For the analysis of data a regression approach was used, building a model representing the sample structure and calculating ε for that model for M photon energies. The calculated values are compared with the measured data in a fit routine that, using a Levenberg–Marquardt algorithm by varying film thickness and optical constants, minimizes the mean squared error, χ^2, defined as:

$$\chi^2 = \frac{1}{2M - P - 1} \sum_{i=1}^{M} \frac{\left(\langle \varepsilon_{1,\text{exp}} \rangle_i - \langle \varepsilon_{1,\text{cal}} \rangle_i \right)^2}{\sigma_{1,i}^2}$$
$$+ \frac{\left(\langle \varepsilon_{2,\text{exp}} \rangle_i - \langle \varepsilon_{2,\text{cal}} \rangle_i \right)^2}{\sigma_{2,i}^2} \quad (2)$$

where M is the total number of data points, P is the number of fitted parameters, $\langle \varepsilon_{1,\text{exp}} \rangle$, $\langle \varepsilon_{1,\text{cal}} \rangle$ and $\langle \varepsilon_{2,\text{exp}} \rangle$, $\langle \varepsilon_{2,\text{cal}} \rangle$ represent the experimental and calculated real and imaginary parts of the pseudodielectric function, and σ_i is the error of each measured quantity.

Films were modeled using either an isotropic model (yielding (n_i, k_i)) and a uniaxial anisotropic layer characterized by the

ordinary (n_o, k_o) out-of-plane refractive index and the extraordinary (n_e, k_e) in-plane refractive index.

Fig. 2 shows typical experimental SE spectra at various angles of incidence for an MEH-PPDFV film deposited on glass. Dots are experimental points and lines are for the fit results according to the model sketched in the same figure. A two-layer model including film and surface roughness was used in the analysis. The surface roughness was modeled using a mixture of 50% of polymer and 50% of voids' dielectric functions. Film thickness was an ellipsometric fitting variable; however, as a starting point of the iterative fitting routine, the film thickness determined independently by stylus profilometry was introduced.

Film morphology and aggregation state were imaged using atomic force microscopy (AFM) in intermittent contact mode (IC-AFM) using an Autoprobe CP-Thermomicroscope. A sharp conical tip with a radius of curvature <10 nm and an amplitude of vibration of 80 kHz (dLever Series Probe) mounted of a p-type doped Si cantilever was used.

Photoluminescence (PL) spectra were recorded at room temperature using an Argon ion (355 nm) laser excitation source at 1 mW excitation power and a photomultiplier as detector.

Electroluminescence (EL) measurements were performed on a device structure consisting of a 120 nm transparent ITO (indium-tin-oxide) layer as the bottom electrode, supported on a glass substrate, a 100 nm PEDOT:PSS layer and an approximately 80 nm emissive layer of the MEH-PPDFV polymer (see scheme in Fig. 7). Poly(3,4-ethylenedioxythiophene):poly(styrenesulfonate) (PEDOT: PSS, 1:6 dispersion in water, electronic grade AI4083) was purchased from HC Starck. The emissive film was dried in vacuum. The barium electrode (5 nm) was evaporated on top of the film in a vacuum chamber at a pressure of 8.0–9.0×10^{-6} Torr at a rate of 5 Å s^{-1}. The aluminum top electrode (100 nm) was then immediately evaporated on top of the barium without reducing the vacuum.
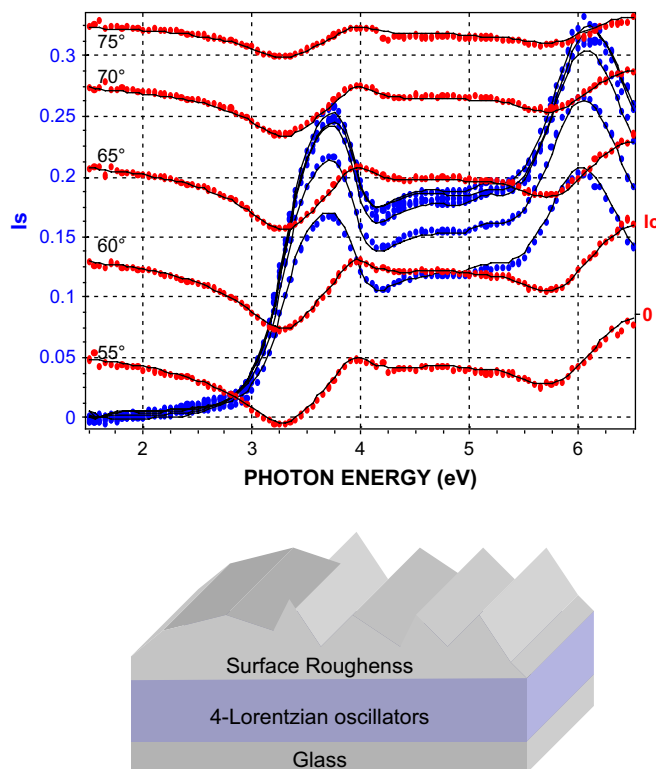

Fig. 2. Typical ellipsometric spectra of the variables Is = sin(2Ψ)sin(2Δ) and Ic = sin(2Ψ)cos(2Δ) at various incidence angles in the range 55°–70° for MEH-PPDFV film of 100 nm (Ψ and Δ are the ellipsometric angles).
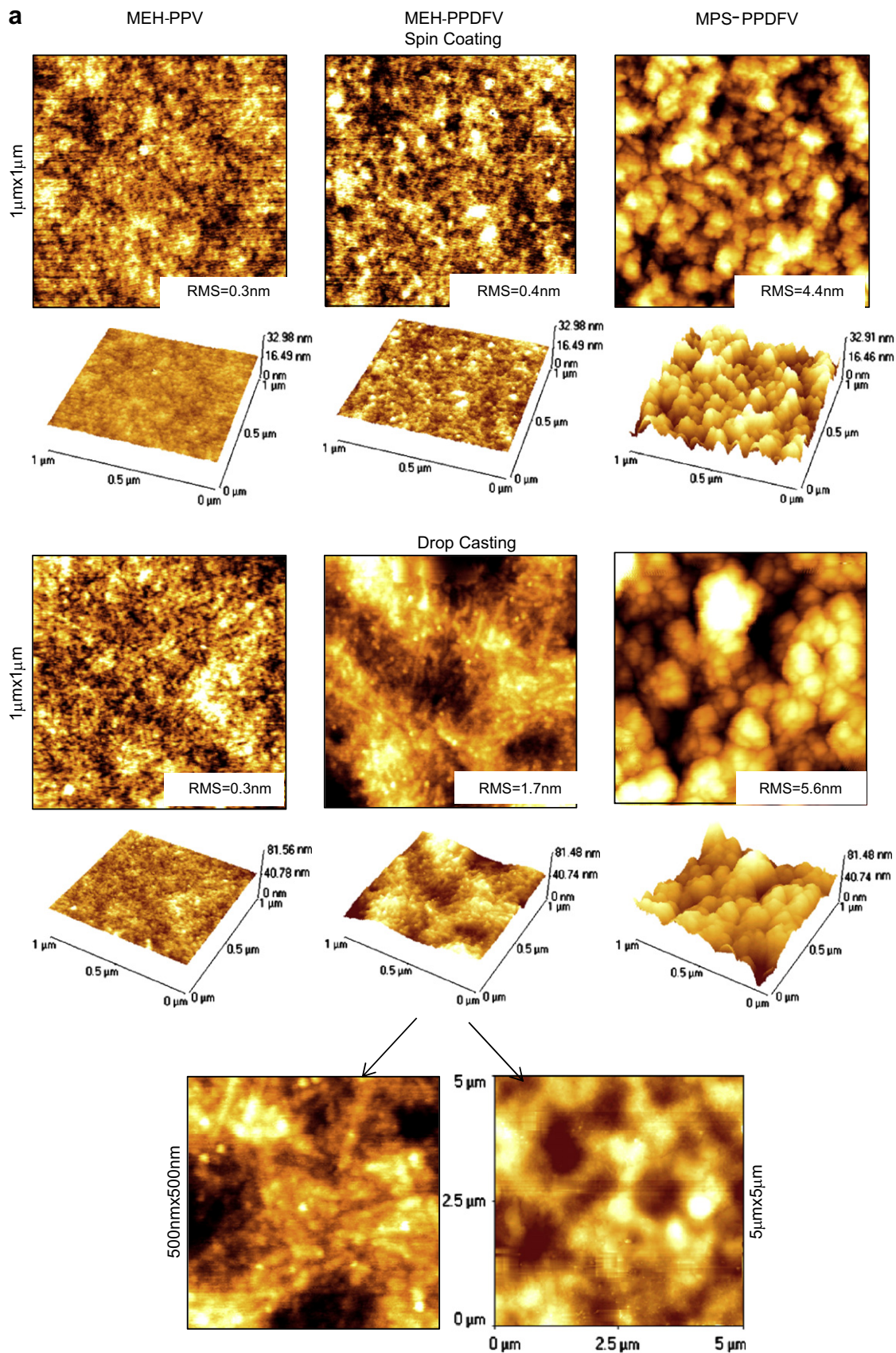
Fig. 3. (a) AFM images of films of the MEH-PPV and of the fluorinated-vinylenes MEH-PPDFVs and of the ionic MPS-PPDFV deposited by both spin coating and casting; (b) thickness dependence of the film morphology and aggregate size for the films of the MPS-PPDFV polymer.
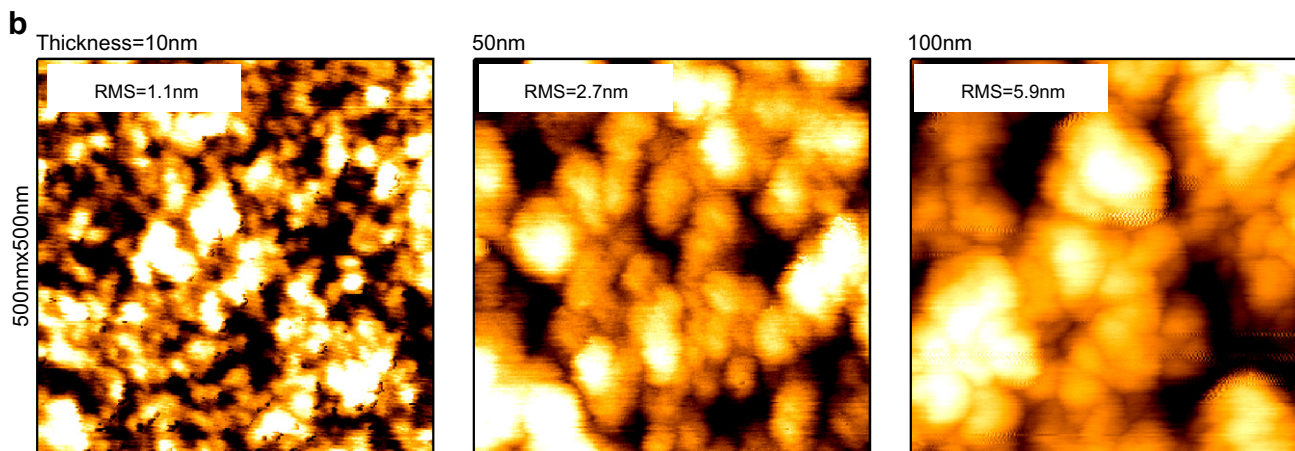
b

Fig. 3. (*continued*).

3. Results and discussion

The organization of polymer chains in the solid state crucially determines properties of polymer thin films. The variability in film microstructure markedly influences the optical characteristics. In a perspective of technological relevance, the interplay between supramolecular organization in the solid state and optical properties needs to be addressed in order to achieve control of thin organic film optical behavior. Therefore, Fig. 3 shows AFM morphologies and corresponding 3D images for thin films obtained by both spin coating and casting for the three polymers. Surface roughness (rms) is also reported, which is also an important parameter that might hinder the movement of charge carriers because can lead to the formation of voids or non-interconnectivity between grains that act as electrical traps. The AFM images show that microstructure and morphology are controlled by both polymer structure and methodology of film preparation. In particular, MEH-PPV forms aligned domains with a size of 100–200 nm by casting, due to inter-chain π-stacking, which also results in a very low surface roughness of approximately 0.3 nm.

The presence of F-atoms in the vinylene units (MEH-PPDFV) strongly impacts on the supramolecular organization and prevents π-stacking between polymeric chains. Spin coating results in the propensity to form randomly disordered and rough films because of rapid evaporation of solvent, whereas casting yields isolated wires' conformation. By casting in controlled atmosphere, the solvent evaporation results in condensation of water droplets that self-organize creating a semi-regular template that, in turn, aids polymer chains to form almost an honeycomb structure, which is more porous (see below discussion on refractive index) [29].

Conversely, the ionic fluorinated high molecular weight polymer MPS-PPDFV forms "granular/nodular" microstructures, where agglomeration and cluster size increase with film thickness as shown in Fig. 3b, due to the low mobility of long polymeric chains and due to the inter-chain interaction induced by the ionic side group. The presence of small granular bumps also for very thin films ($\sim$5 nm) indicates that they stem from aggregates already formed in the solution. This is a hypothesis also consistent with the red-shift of the emission of MPS-PPDFV compared to MEH-PPDFV already observed in solution (λ_{max} MPS-PPDFV = 490 nm vs λ_{max} MEH-PPDFV = 468 nm). This globular morphology results in very rough films.

Correspondingly, different optical properties have been measured by spectroscopic ellipsometry, since supramolecular ordering plays an important role in controlling the optical properties of these materials, as shown by the spectra of the refractive index, n, and of the extinction coefficient, k, reported in Figs. 4 and 5, respectively, in the 0.75–6.5 eV photon energy range. In particular, MEH-PPV films are highly uniaxial anisotropic independent of the film preparation as shown by the spectra of the ordinary, (n_o, k_o) (perpendicular to the film surface), and extraordinary (n_e, k_e) (parallel to the film surface), refractive index and extinction coefficient reported in Figs. 4a and 5a. The present data indicate that optical anisotropy can be observed also for the low M_w of 6500 g/mol for MEH-PPV ordered films, contrarily to what reported in Ref. [30]. The measured birefringence, Δn, is 0.2–0.3 in the transparent region, as expected on the basis of an analysis of the various data present in literature [18,31,32]. Furthermore, data in Fig. 4 indicate that spin coating yields films with a refractive index, and hence, density, higher than casting for all investigated polymers, consistently with morphologies shown in Fig. 3.

From the ratio of the ordinary and extraordinary extinction coefficient values at the maximum of the π–π^* transition, the angular distribution, $d_{\pi\theta}$, can be calculated [33], being 0.83 for the present MEH-PPV films casting-deposited, a value close to the value of 0.84 reported for MEH-PPV with alignment parallel to the substrate surface (plane-on chain conformation) [34], thus indicating the preferential in-plane alignment of MEH-PPV chains. A lower value $d_{\pi\theta} = 0.8$ is determined for films deposited by spin coating, confirming that films by casting are more anisotropic than spin-coated films and that MEH-PPV polymer chains have a tendency for alignment parallel to the substrate.

Similarly, Figs. 4b and 5b show the optical constants of the fluorinated MEH-PPDFV films. In this case, isotropic films are obtained by spin coating while anisotropic films are deposited by casting, consistently with the different morphologies highlighted by AFM in Fig. 3. For MEH-PPDFV, a value of $d_{\pi\theta} = 0.76$ is derived which is lower than that of MEH-PPV because of the distortion introduced in the polymer chain by the fluorine atoms. Conversely, both spin-coated and casted MPS-PPDFV films are isotropic due to the globular morphology, which also results in a thickness dependence of the optical constants.

In addition to morphology and anisotropy, the presence of fluorine atoms on the vinylene units importantly affects the fundamental π–π^* (HOMO–LUMO) transition, as shown by the spectra of the extinction coefficient, k, in Fig. 5. All spectra show a main peak that is due to fundamental π–π^* (HOMO–LUMO) transition of the conjugated backbones, a shoulder due to mixing of several transition involving delocalized levels, and a peak at very high energy (5.96 ± 0.02 eV) due to the π–π^* transition of the benzene units. This last transition is almost the same for all films, since the π–π^* transition of the benzene units is not affected by conjugation length and supramolecular organization.
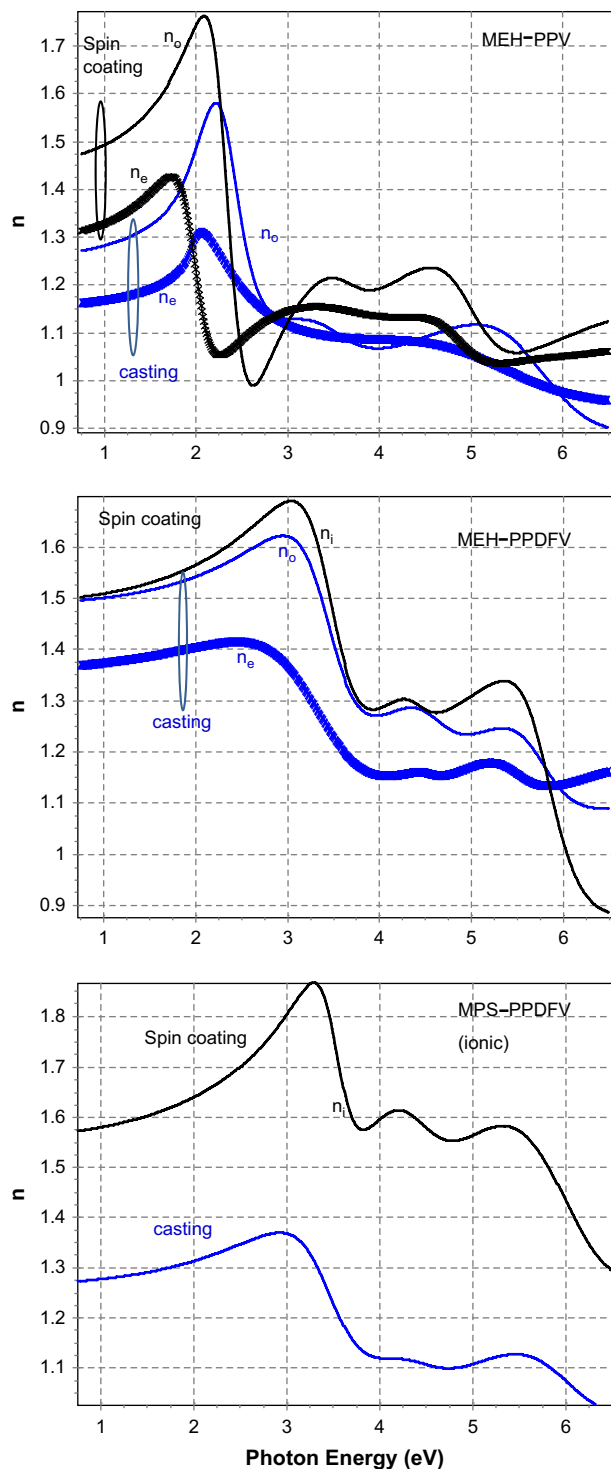
Fig. 4. Spectra of the refractive index of ∼100 nm thick films deposited by spin coating and casting for the MEH-PPV, MEH-PPDFV and MPS-PPDFV polymers. n_i indicates the isotropic refractive index, whereas n_o and n_e are the ordinary and extraordinary refractive indexes of anisotropic films.
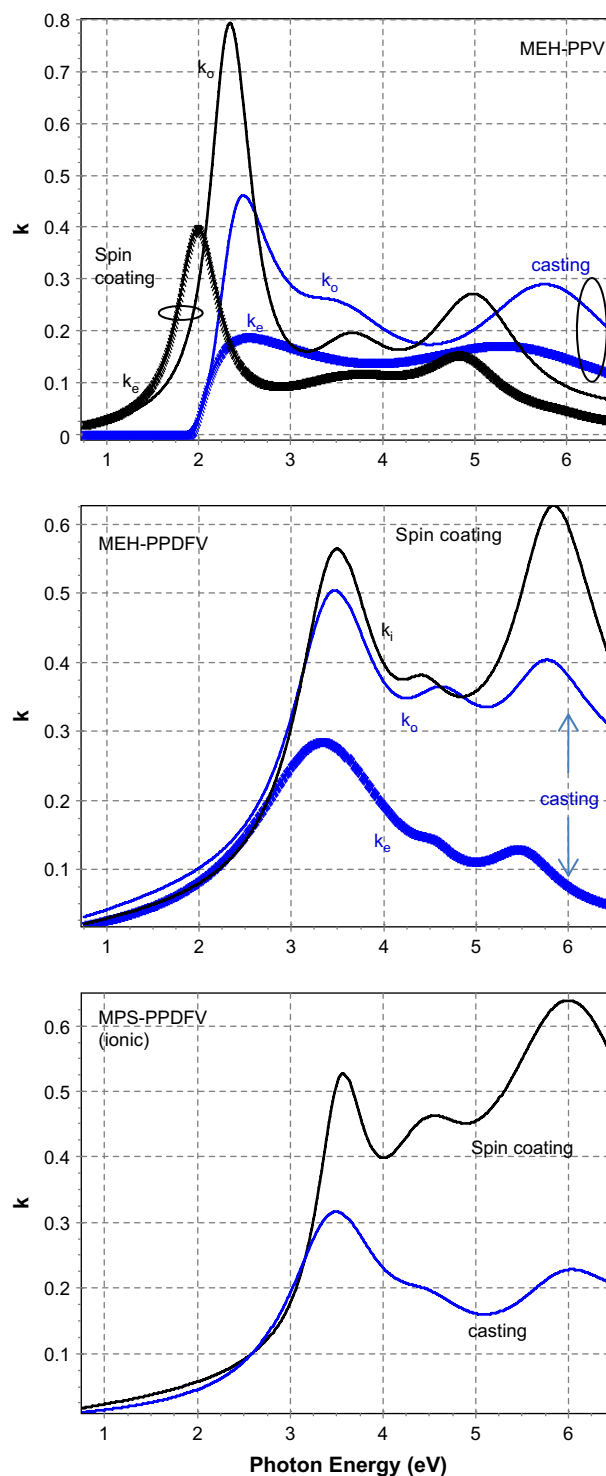
Fig. 5. Spectra of the extinction coefficient of ∼100 nm thick films deposited by spin coating and casting for the MEH-PPV, MEH-PPDFV and MPS-PPDFV polymers. k_i indicates the isotropic extinction coefficient, whereas k_o and k_e are the ordinary and extraordinary extinction coefficients of anisotropic films.

In particular, casted MEH-PPV films show an absorption onset at 2.1 eV, whereas spin-coated films have an extended tail to lower energy due to the higher morphological/microstructural disorder consistently with the lower anisotropy. Furthermore, k spectra exhibit the maximum of the fundamental π–π^* transition peak at 2.33 eV (532 nm), which is red-shifted with respect to the MEH-PPV absorption maximum in solution observed at 480 nm, consistently with the regular π stacks in the solid state.

The presence of F-atoms in the vinylene units, which prevents the regular packing of π stacks, results in a blue-shift of about 200 nm, which is the highest blue-shift reported for PPVs to our knowledge, of the fundamental π–π^* transition from 2.33 eV (for the MEH-PPV) to 3.74 eV (331 nm) for the MEH-PPDFV and to 3.50 eV (354 nm) for MPS-PPDFV. Furthermore, the fundamental π–π^* transition is also blue-shifted with respect to the polymer in solution, where the absorption maximum was observed at 360 nm,

because of the reduction of inter-chain interaction, ascribable to torsion introduced by the fluorine atoms caused by steric repulsion between the fluorine atoms on the vinylene units and the oxygen atoms on the aromatic rings [35].

The above MEH-PPDFV polymeric films show strong blue photoluminescence (PL) at room temperature (see Fig. 6), with a maximum at 2.71 eV (458 nm), which is slightly blue-shifted also with respect to the polymer in chloroform solution (PL λ_{max} at 468 nm), differently from the red-shift of the emission spectrum of MEH-PPV films compared to solution. This blue-shift of the polymer in the solid state with respect to the solution indicates that no strong inter-chain aggregation occurs for the MEH-PPDFV in thin films. Furthermore, the MEH-PPDFV PL λ_{max} is also blue-shifted of about 110 nm relative to that of MEH-PPV. A comparison of the present data with the PL λ_{max} of 495 nm of DMOS-PPDFV reported by Jin et al. [22] underlines a further 37 nm blue-shift for MEH-PPDFV. This blue-shift can be attributed to a torsion of the polymeric chain induced by the fluorine atoms that, in the case of the MEH-PPDFV, interact with two substituents on the aromatic rings rather than one as in the case of the DMSO-PPDFV. This effect, which causes a further reduction of the conjugation length, inhibits planarization and inter-chains' interaction. Furthermore, consistently with the AFM and SE data, the comparison of PL spectra of MEH-PPDFV films from spin coating and casting indicates a shoulder at 2.40 eV (515 nm), which is indicative of the inter-chain interaction in the film, more pronounced for the spin-coated film, whose PL peak is also slightly red-shifted with respect to the casted film. Therefore, it can be inferred that the inter-chain interaction is more effective in films from spin coating than from casting, consistently with the more packed morphology and higher refractive index.

Preliminary data on the electroluminescence (EL) are reported in Fig. 7, which shows the normalized EL spectrum of the ITO/PEDOT/MEH-PPDFV/Ba/Al device. For comparison, the EL spectrum of the MEH-PPV recorded under the same experimental conditions is also reported. The EL spectra of MEH-PPDFV and MEH-PPV exhibit maximum of peaks at 2.46 eV (504 nm) and 1.98 eV (625 nm), which correspond to blue-greenish and red light, showing a blue-shift of 120 nm for the fluorinated MEH-PPDFV.

On the electroluminescence properties and their optimization, further study is in progress focusing on the investigation of the effect of the MEH-PPDFV films' deposition conditions (e.g., polymer concentration, solvent type, film thickness) that modify MEH-PPDFV self-aggregation in the solid state and consequently the emissive properties.
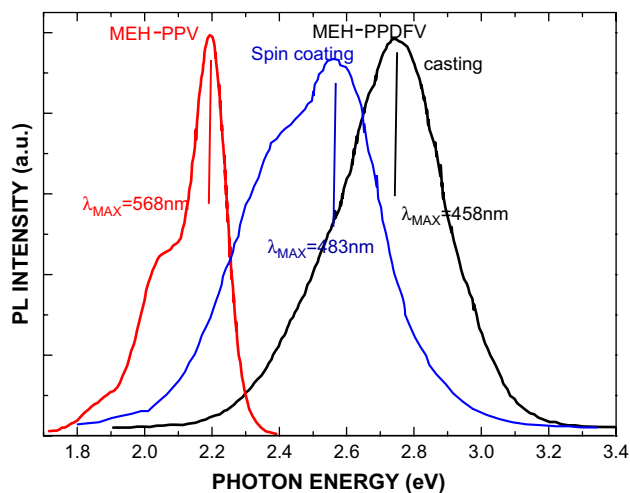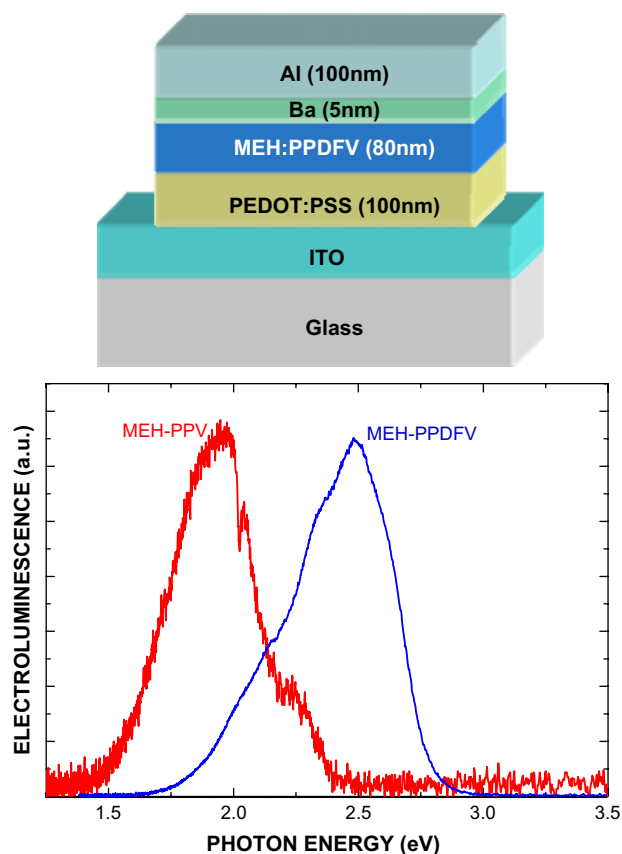

Fig. 7. Electroluminescence spectrum of the device structure using $\sim$80 nm thick films of the MEH-PPDFV polymer as schematized. For comparison a similar device using MEH-PPV film was also measured.

4. Conclusions

The impact of fluorinated vinylene units of MEH-PPDFV and MPS-PPDFV polymers synthesized by the Stille cross-coupling reaction on the self-organization and on the optical properties of thin films prepared by spin coating and casting has been investigated. A comparative analysis with films of MEH-PPV obtained by the same synthetic route has also been presented. The present approach has been based on measurements of the PPDFV dielectric function exploiting spectroscopic ellipsometry, which is well suitable for measuring optical properties and for inferring information on conjugated plane orientation through measurements of optical anisotropy. By ellipsometry and photoluminescence, it has been shown that MEH-PPDFV films show a large blue-shift of the fundamental π–π^* transition observed at 3.74 eV (at 331 nm) as well as of the room temperature blue PL at 2.71 eV (458 nm) in the solid state, which is blue-shifted of 200 nm with respect to the non-fluorinated MEH-PPV. Preliminary electroluminescence data on spin casted films also show a blue-shift of the emission maximum from 1.98 eV (MEH-PPV) to 2.46 eV for the fluorinated MEH-PPV. Although the structure/morphology and supramolecular organization in the solid state require further improvement, it is demonstrated that the value of the π–π^* transition is affected by electronic structural changes associated with changes in self-organization in the solid state induced by the fluorine atoms on the vinylene units, which reduce the conjugation length and inhibit stacking of polymer chains, and that the presence of fluorine atoms on the vinylene units of PPVs represents a valuable way to blue-shift the optical absorption and emission.

Fig. 6. Room temperature photoluminescence spectra of $\sim$100 nm thick films deposited by casting for the MEH-PPV and by casting and spin coating for the MEH-PPDFV polymer.

Acknowledgment

References

[1] Skotheim TA, Reynolds JR, editors. Handbook of conducting polymers. 3rd ed. New York; 2007.
[2] Liu J, Zhou QG, Cheng YX, Geng YH, Wang LX, Ma DG, et al. Adv Funct Mater 2006;16:957.
[3] Martin RE, Geneste F, Riehn R, Chuah BS, Cacialli F, Friend RH, et al. Chem Commun 2000:291.
[4] Martin RE, Geneste F, Chuah BS, Fischmeister C, Ma Y, Holmes AB, et al. Synth Met 2001;122:1.
[5] Hsieh BR, Yu Y, Forsyte EW, Schaaf GM, Feld WA. J Am Chem Soc 1998;120:231.
[6] Ahn T, Jang MS, Shim H-K, Hwang DH, Zyung T. Macromolecules 1999;32:3279.
[7] Babudri F, Farinola GM, Naso F, Ragni R. Chem Commun 2007:1003 and references therein.
[8] Babudri F, Cardone A, Chiavarone L, Ciccarella G, Farinola GM, Naso F, et al. Chem Commun 2001;19:1940.
[9] Bredas JL, Heeger AJ. Chem Phys Lett 1994;217:507.
[10] Babudri F, Cardone A, Chiavarone L, Farinola GM, Naso F, Cassano T, et al. Macromol Chem Phys 2003;204:1621.
[11] Gurge RM, Sarker AM, Lahti PM, Hu B, Karasz FE. Macromolecules 1997;30:8286.
[12] Rhien R, Morgado J, Iqbal R, Moratti SC, Holmes AB, Volta S, et al. Synth Met 2001;124:67.
[13] Li SB. Acta Chim Sinica 2006;64:2509.
[14] Li HC, Lin YP, Chou PT, Cheng YM, Liu RS. Adv Funct Mater 2007;17:520.
[15] McCoy RK, Karasz FE, Sarker A, Lahiti PM. Chem Mater 1991;3:941.
[16] Kang I-N, Lee GJ, Kim DH, Shim HK. Polym Bull 1994;33:89.
[17] Kang I-N, Shim H-K, Zyung T. Chem Mater 1997;9:746.
[18] Babudri F, Cardone A, Farinola GM, Martinelli C, Mendichi R, Naso F, et al. Eur J Org Chem 2008;2008:1977.
[19] Jin Y, Kim J, Song S, Park SH, Lee K, Suh H. Bull Korean Chem Soc 2005;26:855.
[20] Jin Y, Kim J, Lee S, Kim JY, Park SH, Lee K, et al. Macromolecules 2004;37:6711.
[21] Scurlock RD, Wang B, Ogilby PR, Sheats JR, Clough RL. J Am Chem Soc 1995;117:10194.
[22] Jin Y, Jee J, Kim K, Kim J, Song S, Park SH, et al. Polymer 2007;48:1541.
[23] Campoy-Quiles M, Etchegoin PG, Bradley DDC. Phys Rev B 2005;72. 045209(1).
[24] Ramsdale CR, Greenham NC. Adv Mater 2002;14:212.
[25] Losurdo M. Thin Solids Films 2004;301:455.
[26] Losurdo M, Bruno G, Irene EA. J Appl Phys 2003;94:4923.
[27] Miller EK, Yang CY, Heeger AJ. Phys Rev B 2000;62:6889.
[28] [Kirova N, Brazovskii S, Bishop AR. Synth Met 1999;100:29.
[29] Nurmawati MH, Renu R, Ajikumar PK, Sindhu S, Cheong FC, Sow CH, et al. Adv Funct Mater 2006;16:2340.
[30] Koynov K, Bathiar A, Ahn T, Bubeck C, Horhold HH. Appl Phys Lett 2004;84:3792.
[31] Boudrioua A, Hobson PA, Matterson B, Samuel IDW, Barnes WL. Synth Met 2000;545:111.
[32] Tammer M, Monkman AP. Adv Mater 2004;14:210.
[33] McBranch D, Campbell IH, Smith DL, Ferraris JP. Appl Phys Lett 1995;66:1175.
[34] Wei PK, Lin YF, Fann W, Lee YZ, Chen SA. Phys Rev B 2001;63. 045417(1).
[35] Piacenza M, Della Sala F, Farinola GM, Martinelli C, Gigli G. J Phys Chem B 2008;112:2996.